Theoretical investigations on the pressure effects in spin-crossover materials: Reentrant phase transitions and other behavior

Killian Babilotte⊙ and Kamel Boukheddaden⊙*

Université Paris-Saclay, UVSQ, Groupe de la Matière Condensée, UMR CNRS No. 8635,
45 Avenue des Etats Unis, 78035 Versailles, France

Pressure effects have been widely studied in spin-crossover (SCO) solids due to their immediate influence on the thermal dependence of the high-spin (HS) fraction. In most of the cooperative SCO materials, the applied pressure shifts the transition temperatures upward and decreases the thermal hysteresis widths to such an extent that it vanishes at some critical pressure. However, several other unexpected experimental features were found in the literature, showing that the applied pressure may (i) induce an increase of the thermal hysteresis width or even (ii) lead to a reentrant behavior on the thermal hysteresis whose width first increases for low applied pressures and then decreases at high-pressure values. These nonstandard behaviors have been classified as anomalous, even though the transition temperature always increases under pressure. In this theoretical contribution, we rationalize all these behaviors by describing the spin-crossover system under pressure with an elastic description accounting for the difference of lattice parameters between the low-spin (LS) and HS phases including the pressure effects. The analytical study of this elastic model in the homogeneous mechanical system demonstrated its isomorphism with an Ising-like model with infinitely long-range interactions, in which the pressure acts linearly on the ligand field and nonlinearly on the strength of the interactions. The resolution of this model brings to light the existence of a pressure-induced interplay between these two contributions allowing one to recover a wide range of normal and abnormal observed experimental thermal dependences of the spin transition under pressure.

I. INTRODUCTION

Spin-crossover (SCO) compounds which belong to the field of molecular magnetism are typical examples of a first-order phase transition with hysteresis loop [1–3]. Fe(II) based SCO complexes are among the most studied switchable molecular materials in which the spin transition takes place between two spin states, namely, the high-spin (HS) state, stable at high temperature, and the low-spin (LS) state, which is stable at lower temperature. In the former state, the electrons of the d^6 electronic configuration occupy all orbitals ($t_{2g}^4 e_g^2$) according to the Hund rule and the spin moment reaches its maximum value ($S = 2$), while in the latter state the six electrons occupy the fundamental state ($t_{2g}^6 e_g^0$), thus leading to a null spin moment ($S = 0$). Since the e_g (t_{2g}) orbital is known as the antibonding (bonding) orbital, it follows that in the HS state the bonding between the Fe and the surrounding nitrogen atoms is weakened, which leads to the increase of the Fe-ligand distance by ∼10% compared to that of the LS state, causing a local volume expansion [4,5]. From the elastic rigidity point of view, the SCO materials are then softer and more distortable in the HS state than in the LS. It is important to mention for the nonspecialist reader that the SCO solids are paramagnetic in the HS state and diamagnetic in the LS state. One should mention that the main reason for the absence of

magnetic ordering in the HS phase of SCO solids is the lack of covalent bonding between the metal ions, which are separated by large distances (∼1 nm). Only a few experimental data obtained on the bimetallic coordination polymeric compound [6] have shown the existence of long-range magnetic order which has been modeled using three state spin Hamiltonians [7,8]. From the experimental point of view, the spin transition can be triggered by various external stimuli, such as pressure, light, and temperature [9,10]. The spin transition is intrinsically a vibronic problem [11–14] in which the electronic and vibrational structures of the molecule are strongly intricate. The change of the magnetic state of the metal center is accompanied with local volume changes at the molecular level, which delocalizes far from the epicenter of the transformation (long-range interaction), a result of the elastic interactions between the SCO units, leading to a macroscopic volume change, stabilizing the LS and HS phases at low and high temperature, respectively. These large volume and electronic changes affect significantly the physical properties of the SCO materials, such as color, mechanical properties, etc. Due to the so-important changes, several experimental techniques were used to monitor and study this phenomenon, such as differential scanning calorimetry [15], magnetometry [16], x-ray diffraction [17], Mössbauer spectroscopy [18], diffuse reflectivity [19], optical microscopy [19–25], and quite recently, photoluminescence for the luminescent SCO materials which showed clear correlation between the spin state changes and the luminescence properties [26–29]. Here, we are mostly

*kamel.boukheddaden@uvsq.fr

interested by the pressure dependence of the SCO materials, to which several experimental studies have been devoted, and demonstrated that the SCO materials can be considered as pressure sensors [30–34]. In addition, recent theoretical and experimental analyses have also reported their potential giant barocaloric character, opening the way to possible applications in refrigeration technique [35–38].

From the experimental side, the effect of pressure on the SCO materials has been investigated using various experimental techniques [4,39–59], with the aim to (i) realize piezo switchable SCO materials, and (ii) clarify the interplay between the pressure and the thermal properties of the SCO solids. It is observed that depending on the studied SCO sample under pressure, the thermal hysteresis width may decrease (in most of the cases) or increase, and in some cases reentrant behaviors are even observed [60]. In contrast, in all cases the transition temperature from LS to HS is shifted to higher values, as a result of the increase of the local ligand-field strength. Another complexity generated by the applied pressure is the possible pressure-induced crystallographic transitions which then alter the intermolecular packing, or which even lead to symmetry breaking [60–67]. However, one should mention that this last case remains quite rare and most of the transformations are isostructural.

From the theoretical point of view, several models have been proposed to explain the effect of pressure [68–81]. Some of them were based on an Ising-like description where the pressure effect was introduced mostly in the ligand-field energy; others based on more sophisticated elastic descriptions of continuum mechanics considered the effect of anisotropic pressure on the lattice. On the other hand, recent discrete elastic models have also been used to study the effect of pressure on SCO materials, leading to finding a part of the set of rich variety of experimental results reported in the literature.

In the current study, we present an original elastic model for spin-crossover materials which includes the effect of pressure. A detailed analysis of this model allowed us to demonstrate, that in mechanical equilibrium, this model becomes equivalent to an Ising-like Hamiltonian with an effective infinitely long-range interaction. This way, we could identify the elastic nature of the Ising-like interaction parameter and we have been able to determine the pressure dependences of the ligand-field and the effective Ising interaction. We considered here the specific case of "ferromagneticlike" interacting spin-crossover molecules, leading to thermal hysteresis, although the model can be extended as well to include the situations of two-step transitions [80] with the presence of an intermediate plateau along the spin transition. Since an Ising model with infinitely long range is equivalent with the mean-field Hamiltonian, we have resolved analytically all thermal dependences of the HS fraction with temperature for various pressure and clarified the conditions of obtaining normal and abnormal pressure dependence of the thermal hysteresis widths. The manuscript is organized as follows: In Sec. II, we introduce the elastic modeling of the spin transition, from which we derive the Ising-like description. Section III summarizes the various thermal behaviors of the high-spin fraction under pressure, according to the effect of pressure on the ligand-field and interaction parameters. In Sec. IV,

we conclude and outline the possible developments of this work.

II. THEORETICAL DESCRIPTION

Relevant microscopic models describing the SCO transition are usually elastic models [68–81]. Although very efficient in reproducing the main temperature and spatiotemporal dependences of SCO materials, they are very heavy to handle analytically and can be solved only by combining Monte Carlo simulations and molecular dynamics methods. Here, we show that these models can be reformulated as Ising-like models, whose analytical treatment is more accessible, especially for discussing the effect of pressure on the switchable SCO solids.

A. Derivation of the Ising-like model from an elastic description

An electroelastic model describing the SCO phenomenon combines the spin state and volume changes along the spin transition. Let us consider for simplicity a two-dimensional (2D) elastic SCO lattice, constituted of SCO sites connected by springs. The total potential energy of the system contains two contributions, arising from (i) the electronic local ligand field acting on each spin-crossover site and (ii) the elastic interaction between neighboring molecules. A simple model allowing us to mimic accurately the SCO phenomenon is based on the description of the SCO molecule by a two-state fictitious spin, s, whose eigenvalues $s = -1$ and $s = +1$ are, respectively, associated with the LS and the HS states. Due to the difference of the spin states of the molecule between the LS and HS states, and to the volume expansion in the HS state, the vibrational properties of the lattice are significantly altered. As a result, the HS state is softer than the LS state, and so the phonon spectra in HS have a lower frequency compared to those of the rigid LS phase. As a direct consequence, this confers to the HS state a higher effective degeneracy, $g_{HS} \gg g_{LS}$. At 0 K, the LS state is stabilized by the ligand-field energy Δ_0 arising from the close nitrogen atoms surrounding the Fe(II) metal. On the other hand, the volume change at the spin transition imposes the consideration of different lattice parameters between the LS and the HS phases. Let us consider two neighboring spin sites (i and j); their electronic configurations can be HS-HS, HS-LS, or HS-LS (LS-HS), to which correspond the respective bond length distances, a_{HH}, a_{LL}, and a_{HL} ($= a_{LH}$). Here, we clearly have $a_{LL} < a_{HL} < a_{HH}$. In addition, for simplicity reasons, we will consider that the equilibrium bond length for HS-LS configuration is such that $a_{HL} = \frac{a_{HH} + a_{LL}}{2}$. Let us notice by x_{ij} the instantaneous distance between these two sites. Then, in the harmonic approach, the elastic Hamiltonian describing this SCO lattice is simply

$$H = \frac{K}{2} \sum_{ij} (x_{ij} - a_{ij})^2 + \Delta_{eff} \sum_i s_i, \qquad (1)$$

where K is the elastic constant, assumed here as independent of the spin states. Here, the next-nearest neighbors are omitted for clarity. To ensure the dependence of the equilibrium bond length on the spin states, s_i and s_j, a_{ij} are expressed as a

function of s_i and s_j as follows:

$$a_{ij} = a_{\mathrm{HL}} + \frac{\delta a}{4}(s_i + s_j), \qquad (2)$$

where $\delta a = a_{\mathrm{HH}} - a_{\mathrm{LL}}$ is the lattice parameter misfit between the HS and LS phases.

In Eq. (1), the fieldlike term Δ_{eff} represents the effective energy gap,

$$\Delta_{\mathrm{eff}} = \Delta_0 - k_B T \ln g, \qquad (3)$$

which contains the contributions of the ligand-field energy Δ_0 and the degeneracies ratio, $g = g_{\mathrm{HS}}/g_{\mathrm{LS}}$, between the LS and HS states, which clearly plays the role of an entropic term ($k_B \ln g$,). The variable T is the temperature.

A simple method to solve this problem consists in considering a homogeneous elastic system, i.e., by taking $x_{ij} = x$, which is now space invariant. The total elastic energy (1) becomes $E = \frac{K}{2} \sum_{ij} (x - a_{ij})^2 + \Delta_{\mathrm{eff}} \sum_i s_i$. We then look for the minimum elastic energy, by solving $\frac{\partial E}{\partial x} = 0$, which leads to

$$x_{eq} = a_{\mathrm{HL}} + \frac{1}{N}\frac{\delta a}{4} \sum_{ij}(s_i + s_j), \qquad (4)$$

where N is the number of lattice sites. It is interesting to see that the equilibrium lattice spacing, x_{eq}, is written as a function of the average spin state parameter, $m = \langle s \rangle$, as follows,

$$x_{eq} = a_{\mathrm{HL}} + z\frac{\delta a}{8}m, \qquad (5)$$

where z is the coordination number of the lattice, which depends on its topology and symmetry. Inserting now the expression of the equilibrium bond length (5) into Hamiltonian (1), one can easily find that Hamiltonian (1) can be mapped, after some simple algebra, under the form of an Ising-like model, combining short-range and infinitely long-range interactions, whose expression is given by

$$H = h\sum_i^N s_i - J_0 m \sum_i s_i - J' \sum_{ij} s_i s_j + C, \qquad (6)$$

where c is a constant and the fieldlike, h, and exchangelike terms are written as

$$h = \Delta_{\mathrm{eff}},$$
$$J_0 = \frac{z^2 K(\delta a)^2}{8}, \qquad (7)$$
$$J' = -\frac{K(\delta a)^2}{8}.$$

It is worth mentioning that the present calculations lead to a situation of competing interactions, between "ferromagneticlike" long-range interactions ($J_0 > 0$) and "antiferromagneticlike" short-range interactions ($J' < 0$), although the latter are significantly smaller. Indeed, in the case of a 2D system, $z = 4$, and then J' can be considered as 16 times smaller than J_0, which is then omitted, for simplicity, in the present study. Finally, the electroelastic Hamiltonian (1) is isomorphic with

the mean-field Ising-like Hamiltonian,

$$H = \Delta_{\mathrm{eff}} \sum_i^N s_i - J_0 m \sum_i s_i. \qquad (8)$$

The SCO phenomenon can be then described using the well-known Ising-like [38–40] model, widely used in the literature to describe the equilibrium and nonequilibrium properties. The most interesting points here are (i) the identification of the elastic origin of the Ising-like parameter J_0, which is proportional to the misfit elastic energy $\frac{K}{2}(a_{\mathrm{HH}} - a_{\mathrm{LL}})^2$, on the one hand, and (ii) its ferrodistortive nature, on the other hand. It is then important to mention that, in the usual Ising model, the term J_0 has nothing to do with the usual magnetic exchange interaction of the Ising model used in magnetism.

B. Analysis of the mean-field results

The analysis of Hamiltonian (8), which is exactly equivalent to that of mean-field theory, leads quite easily to the following homogeneous, free energy:

$$F_{\mathrm{hom}} = \frac{1}{2}J_0 m^2 - k_B T \ln\left[\left(2g \cosh \frac{J_0 m - \Delta_{\mathrm{eff}}}{k_B T}\right)\right], \qquad (9)$$

where $m = \langle s \rangle$ is the average fictitious magnetization per site. Here, z is the lattice coordination number. From the analytical expression of the free energy, given in Eq. (9), one can derive straightforwardly the following self-consistent equation, through the relation $\frac{\partial F_{\mathrm{hom}}}{\partial m} = 0$,

$$m = \tanh \beta [J_0 m - \Delta_{\mathrm{eff}}], \qquad (10)$$

where $\beta = \frac{1}{k_B T}$.

Equation (10) can be reversed so as to express the temperature as a function of the magnetization, which leads to

$$k_B T = \frac{2(\Delta_0 - Jm)}{\ln\left(g^2 \frac{1-m}{1+m}\right)}, \qquad (11)$$

which allows plotting directly the magnetization m vs the temperature T without solving any self-consistent equation. The HS fraction (n_{HS}), which is the fraction of molecules occupying the HS state, is simply related to the fictitious magnetization as

$$n_{\mathrm{HS}} = \frac{1 + m}{2}. \qquad (12)$$

A brief look at Eqs. (10) and (11) shows that $m = 0$ is always a solution when $\Delta_{\mathrm{eff}} = \Delta_0 - k_B T \ln g = 0$. Once $m = 0$, the HS fraction value is $n_{\mathrm{HS}} = \frac{1}{2}$, which means that the temperature cancelling the effective field is the transition equilibrium temperature of the system, the expression of which is written as

$$T_{eq}^0 = \frac{\Delta_0}{k_B \ln g}. \qquad (13)$$

Without going into further details, we mention that the phase diagram of the present model is very simple: (i) a first-order spin transition with a thermal hysteresis is obtained when the Curie temperature $T_C^0 = \frac{J_0}{k_B}$ (in mean field) of the associated pure Ising model, i.e., without field ($\Delta_0 = 0$ and $g = 1$), is such that $T_C^0 > T_{eq}^0$, while (ii) the gradual spin conversion takes place otherwise.
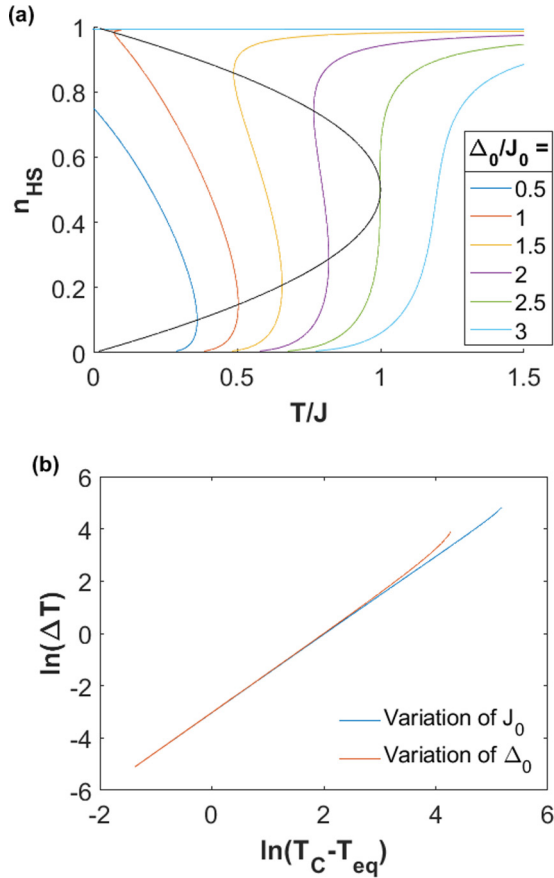
FIG. 1. (a) Thermal dependence of the HS fraction for different values of the ratio $\frac{J_0}{\Delta_0}$, showing the presence of a critical point for $\Delta_0 = J_0$. The spinodal curve, given by Eq. (16), is superimposed for clarity reasons. (b) $\ln(\Delta T)$ vs $\ln(T_C - T_{eq})$ showing a linear dependence, with a slope $\frac{3}{2}$, following the power law given by Eq. (17). In (b) J_0 (Δ_0) is fixed to 120 K (300 K) when Δ_0 (J_0) is varied. The other parameters values used are $g = \sqrt{150}$.

In Fig. 1(a), we depict the effect of the ratio $\frac{\Delta_0}{J_0}$ between the ligand-field energy Δ_0 and the interaction parameter J_0 on the thermal dependence of the HS fraction. We clearly see that when J_0 is below the threshold value, $J_C^0 = \frac{\Delta_0}{k_B \ln g}$, which corresponds to $T_C^0 = T_{eq}^0$, the transition between the LS and HS states is gradual, while above this value, it takes place through a first-order transition accompanied with a thermal hysteresis, the width of which, $\Delta T_0 = T^+ - T^-$ (T^+ and T^- are, respectively, the upper and lower transition temperatures of the thermal hysteresis,) increases with the interaction J_0 and decreases with increasing the ligand field Δ_0.

It is interesting to mention that the spinodal points of the coordinates (T^+, m^+) and (T^-, m^-) of the thermal hysteresis can be found after solving the equation $\frac{\partial T}{\partial m} = 0$. The analytical calculations give, for $\frac{\partial T}{\partial m}$, the following expression:

$$\frac{\partial k_B T}{\partial m} = \frac{4 \frac{\Delta_0 - Jm}{(1-m^2)} - 2J \ln \left(g^2 \frac{1-m}{1+m} \right)}{\left[\ln \left(g^2 \frac{1-m}{1+m} \right) \right]^2}. \quad (14)$$

An interesting piece of information, derived from Eq. (14), concerns the slope $\frac{\partial T}{\partial m}$ at $m = 0$, noted $\frac{\partial T}{\partial m}|_0$, whose

expression is

$$\left. \frac{\partial T}{\partial m} \right|_0 = \frac{T_{eq}^0 - T_C^0}{r}, \quad (15)$$

where $r = \ln(g)$. The slope $\frac{\partial T}{\partial m}|_0$ is expected to be positive for a gradual spin transition and negative in the case of a first-order transition, as clearly depicted in Fig. 1(a). These last two conditions are exactly those corresponding to the existence or not of a first-order transition within this model: A negative slope leading to a first-order transition is possible for $T_{eq}^0 < T_C^0$ and a positive slope leading to a gradual spin-crossover transition requires having $T_{eq}^0 > T_C^0$.

C. Spinodal curve

The spinodal curve, which is the trajectory of the set of solutions (m^+, T^+) and (m^-, T^-) corresponding to the upper and lower branches of the thermal hysteresis in the coordinate frame (m, T), is obtained by combining Eq. (15) for $\frac{\partial T}{\partial m} = 0$ with Eq. (14) and gives the simple relation

$$T = T_C(1 - m^2), \quad (16)$$

where $T_C = \frac{J_0}{k_B}$. The spinodal curve is represented in Fig. 1(a) as a parabola in the referential frame (T, m) for the maximum temperature value $T = T_C$ obtained for $m = 0$ and delimits the space of coordinates where the system admits a thermal hysteresis. Knowing that at $m = 0$, the temperature is $T = T_{eq}$, corresponding to the transition temperature, then the existence of the thermal bistability is again found here as $T_{eq} < T_C$, in excellent agreement with the analysis made on the sign of the slope $\frac{\partial T}{\partial m}|_{m=0}$.

The meticulous inspection of the dependence of the thermal hysteresis on the quantity $T_C - T_{eq}$, shown in Fig. 1(b)–in the bistable region, the distance on the quantity $(T_C^0 - T_{eq}^0)$, which represents the gap between the transition temperature and the Curie temperature (T_C) above which the thermal hysteresis vanishes–leads to the following universal power law,

$$\Delta T \sim \left(T_C^0 - T_{eq}^0 \right)^{3/2}, \quad (17)$$

which holds for both dependencies of ΔT, on the interaction parameter J_0 and the ligand field Δ_0, as clearly depicted in Fig. 1(b).

III. PRESSURE EFFECTS

To consider the pressure effects in SCO materials, one has to come back to the elastic Hamiltonian (1). It is expected that the effect of pressure on the elastic Hamiltonian will renormalize the elastic constant K and will affect the connectivity of the lattice z as well as the total elastic energy. As for the elastic constant, it is clear that the pressure will enhance the rigidity of the LS and HS states, which then results in the increase of the bulk modulus as well as the shift of the phonon spectrum. On the other hand the change in connectivity is mainly due to the molecular structure of the SCO materials, and therefore under pressure new steric contacts (hydrogen-hydrogen contacts, π-π stacking, etc.) will be strengthened or weakened. For simplicity reasons, and without losing the general character of the phenomenon, we

perform the following developments on a one-dimensional (1D) SCO chain. The elastic Hamiltonian of the chain under pressure P is written as

$$H = \frac{K(P)}{2} \sum_{ij} (x_{ij} - a_{ij})^2 + \Delta_{\text{eff}} \sum_i s_i + P \sum_{ij} x_{ij}, \quad (18)$$

where in the last term, the quantity $\sum_{ij} x_{ij}$, represents the length of the chain. Using the same procedure as in Sec. II A, by considering a homogeneous bond length $x_{ij} = x$ along the lattice, and minimizing the obtained total elastic energy with respect to the x variable, the bond length at mechanical equilibrium becomes

$$x_{eq} = a_{\text{HL}} + z \frac{\delta a}{8} m - \frac{P}{K}. \quad (19)$$

Equation (19) shows, as expected, that under pressure the bond length reduces by the quantity $-\frac{P}{K}$, indicating a contraction of the system's volume (here length). Inserting now expression (19) in Hamiltonian (18) and after conducting all calculations, we arrive to the following effective Ising-like Hamiltonian,

$$H = \left(\Delta_0 - k_B T \ln g + P \frac{\delta a}{2} \right) \sum_i^N s_i - J(P) m \sum_i s_i + c(m, P), \quad (20)$$

where $(\Delta_0 - k_B T \ln g + P \frac{\delta a}{2})$ is the new ligand-field energy; $J(P) = \frac{z^2 K (\delta a)^2}{8}$ is the interaction parameter; and $c(m, P)$ is a term which depends on the average fictitious magnetization m and pressure P, which does not play any role in the thermodynamic properties because it does not depend on the spin states.

According to Hamiltonian (20), the pressure influences both the initial ligand field, $\Delta_{\text{eff}} = \Delta_0 - k_B T \ln g$, and the Ising-like interaction J_0. Interestingly, the pressure renormalizes linearly the ligand-field energy in which an additional positive term, $P \frac{\delta a}{2}$, emerges, thus increasing the energy gap between the LS and the HS states. This is in excellent agreement with experimental results which indicate that the transition temperature of SCO complexes increases linearly with the pressure, as will be discussed below.

While the effect of pressure on the ligand field is quite clear, its consequence on the interactions is less evident, because the pressure can lead to the rearrangement of the topology of the network interactions and also can change the shape of the molecules. As a result, the pressure's influence on the interaction parameter J_0 can be nonmonotonous. Indeed, considering that both elastic constant K and the coordination number z are influenced by the applied pressure, the effective interaction parameter $J_0(P) = \frac{z^2 K (\delta a)^2}{8}$ may depend linearly or nonlinearly on pressure, even by considering linear dependences for $K(P)$ and $z(P)$. It is worth noticing that, even without considering a change in the lattice coordination number $z(P)$, which requires the precise knowledge of the pressure-induced structural changes, the pressure dependence of the bulk modulus $K(P)$ can be highly nonlinear in solids involving strong deformations or plasticity, and cause a significant enhancement of the effective interaction parameter $J_0(P)$.

All conclusions drawn in the previous section, Sec. II, remain valid under pressure. In particular, the transition temperature $T_{eq}(P)$ still corresponds to the temperature which cancels the effective ligand field. Similarly, the associated Curie temperature, $T_C(P)$, of the second-order phase transition remains that of the mean field. Thus, $T_{eq}(P)$ and $T_C(P)$ are given by the following expressions:

$$T_{eq}(P) = T_{eq}^0 + \frac{\delta a}{2 k_B \ln g} \quad \text{and} \quad T_C(P) = \frac{J(P)}{k_B} = \frac{z^2 K (\delta a)^2}{8 k_B}. \quad (21)$$

Let us first discuss the pressure effect on the ligand field. From the experimental point of view, except for one or two experimental cases [78], almost all experimental examples of SCO materials under pressure demonstrated that the transition temperature, $T_{eq}(P)$, of the materials linearly increases with the applied pressure P following the Clausius-Clapeyron law,

$$T_{eq}(P) = T_{eq}^0 - (P - P_{atm}) \frac{\Delta V}{\Delta S}, \quad (22)$$

where $\Delta V (< 0)$ is the volume change between HS and LS states, ΔS is the associated entropy change, and P_{atm} is the ambient pressure, which will be absorbed in P in the developments below. It is interesting to notice that from the experimental point of view that the ratio $\frac{\Delta V}{\Delta S}$ is evaluated to $|\frac{\Delta V}{\Delta S}| \sim 19 - 20$ K kbar^{-1}, for the molecular SCO compound [Fe(btr)$_2$(NCS)$_2$] H$_2$O [31], while this ratio is of about 30 K kbar^{-1} for switchable Prussian blue analogs [32,33], which have a less rigid lattice due to their covalent nature.

According to Hamiltonian (20), the total effective ligand-field energy depends linearly on the pressure. In addition, if one considers a linear relation for the coordination number $z(P)$ and the elastic constant $K(P)$, the effective interaction $J(P)$ can be expanded until the second order with respect to pressure, and thus the following relations can be established:

$$\Delta = \Delta_0 + \alpha P \quad \text{and} \quad J = J_0 + \gamma P + \delta P^2, \quad (23)$$

where α is strictly positive while in general the factors γ and δ can be positive or negative, which means that the pressure can strengthen or weaken the long-range interactions.

The spin transition temperature $T_{eq}(P)$ and the associated Curie temperature $T_C(P)$ of the second-order phase transition is written now as

$$T_{eq}(P) = T_{eq}^0 + \frac{\alpha}{k_B \ln g} P \quad \text{and} \quad T_C(P) = T_C^0 + \gamma P + \frac{\delta}{2} P^2. \quad (24)$$

Using the same procedure as that developed in Sec. II A, we can state that under pressure, the thermally induced spin transition is of first order for $T_C(P) > T_{eq}(P)$ and gradual when $T_C(P) < T_{eq}(P)$.

Thus, according to α, γ, δ, T_{eq}^0, and T_C^0 values, several behaviors of the thermal dependence of the HS fraction under pressure are possible. These behaviors can be classified into two possible situations, corresponding to $T_{eq}^0 < T_C^0$ and $T_{eq}^0 > T_C^0$.

A. Case of hysteretic system at zero pressure: $\delta = 0$ and $T_{eq}^0 < T_C^0$

This first case considers that the studied system exhibits a thermal hysteresis at pressure zero; a condition which is fulfilled for, $T_{eq}^0 < T_C^0$. Then according to the slopes $\frac{\alpha}{k_B \ln g}$ and γ, the effect of pressure may lead to enhance the thermal hysteresis width or to decrease it until it vanishes. In experiments, the first case where the hysteresis width decreases with increasing pressure is very frequent and can be considered as the general rule, which can be easily derived from theory. In contrast, the second case where the thermal hysteresis increases with increasing pressure is considered as an anomalous behavior. The first anomalous increase of the thermal hysteresis under pressure was reported by König *et al.* [79] more than 40 years ago. The existence of these nonstandard behaviors has been confirmed later, by other groups [32], who observed a variety of behaviors, such as hysteresis under pressure which shifts at constant width to higher transition temperatures [80], or vanishing small hysteresis which reappears at higher pressure [81], which could be described as a reentrant phenomenon. Our goal here is to demonstrate that the present model can reproduce a large panel of these behaviors.

1. Case $\alpha > \gamma \ln g$

The classical case, where the applied pressure induces a linear decrease of the thermal hysteresis width is obtained [Fig. 2(a)] when the following condition, $\frac{\partial T_{eq}(P)}{\partial P} > \frac{\partial T_C(P)}{\partial P}$, is realized. In most of the previous Ising models simulating SCO materials under pressure, the pressure was only introduced in the ligand-field contribution, which corresponds to the case $\gamma = 0$, which is included. According to Eq. (22), the condition $\frac{\partial T_{eq}(P)}{\partial P} > \frac{\partial T_C(P)}{\partial P}$ leads to $\alpha > \gamma \ln g$. Figure 2(b) displays the pressure dependence of $T_{eq}(P)$ and $T_C(P)$ in this case; it also constitutes the phase diagram of the system. Indeed, it is expected that for $T_{eq}(P) < T_C(P)$, the HS fraction exhibits a first-order phase transition with a thermal hysteresis, which turns to a gradual transition for $T_{eq}(P) \geqslant T_C(P)$. According to this statement, the thermal hysteresis vanishes at the critical pressure, $P_C = \frac{k_B(T_C^0 - T_{eq}^0)}{(\frac{\alpha}{\ln g} - \gamma)}$. Using the numerical values, $\alpha = 40.1$, $\gamma = 4$ K/kbar, $\sqrt{g} = 150$, $\Delta_0 = 300.6$ K, and $J_0 = 160$ K, the critical pressure P_C is evaluated as ~ 10 kbar, which is in excellent agreement with the thermal dependence behavior of the HS fraction reported in Fig. 2(b). Moreover, the analysis of the dependence of the thermal hysteresis width ΔT as a function of the difference $[T_C(P) - T_{eq}(P)]$ showed the existence of a universal law, as indicated in Fig. 3(c), where a linear plot of ΔT vs $[T_C(P) - T_{eq}(P)]^{\frac{3}{2}}$ is shown, where the pressure becomes a hidden variable.

2. Case $\alpha = \gamma \ln g$

In the special situation where the slopes of the spin transition (T_{eq}) and Curie (T_C) temperatures with pressure are equal, i.e., $\frac{\partial T_{eq}(P)}{\partial P} = \frac{\partial T_C(P)}{\partial P}$, leads to a phase diagram $T(P)$, made of two parallel lines. As a result the "distance" between the two temperatures remains constant and the pressure does not act on the thermal hysteresis width, which remains constant, even though the whole hysteresis shifts
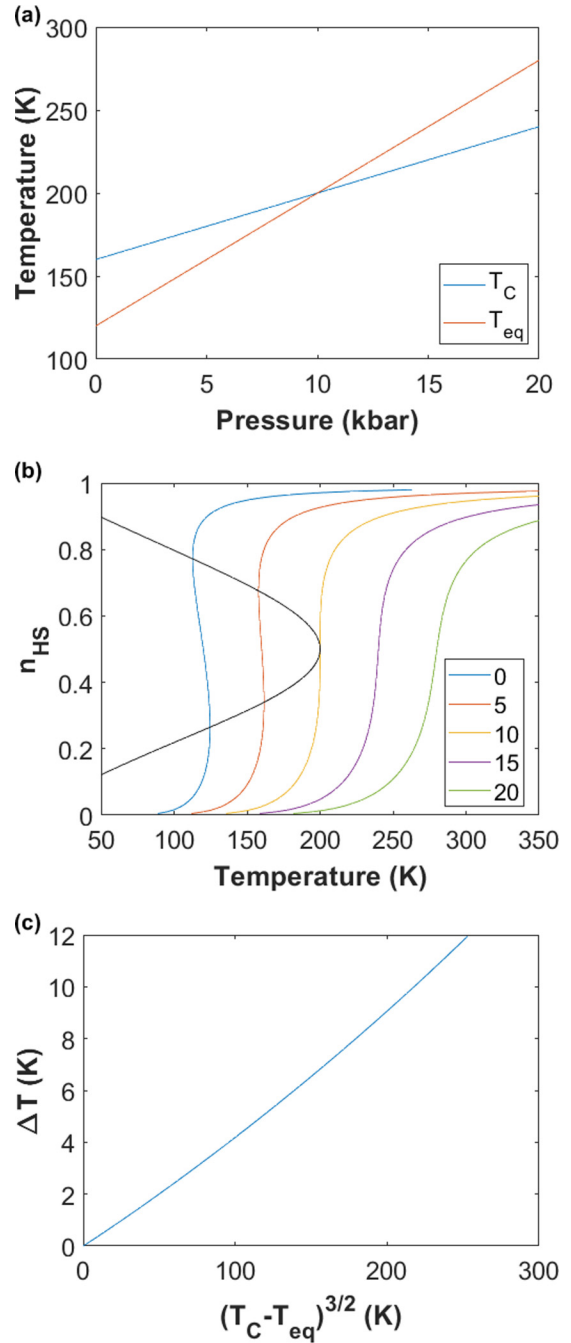

FIG. 2. (a) phase diagram exhibiting the pressure dependence of the spin transition T_{eq} and the Curie temperature T_C. (b) The thermal dependence of the HS fraction under pressure showing the transformation from first-order to gradual spin transition as the pressure increases. The black curve is the spinodal curve, which delimits the bistable region. (c) The superlinear behavior of the thermal hysteresis width as a function of $(T_C - T_{eq})^{3/2}$ obtained for the curves of (a). The parameter values are $\sqrt{g} = 150$, $\Delta_0 = 300.6$ K, $J_0 = 160$ K, $\alpha = 40.1$ K/kbar, and $\gamma = 4$ K/kbar.

to higher-temperature regions. This very particular situation, realized here when $\alpha \approx \gamma \ln g$, has been already reported in the experimental literature, as in the case of the spin-crossover complex [Fe(hyetrz)$_3$](3-nitrophenylsulfonate)$_2 \cdot$ 3H$_2$O (1 $\cdot$ 3H$_2$O), with hyetrz = 4-(2′-hydroxyethyl)-1,2,4-
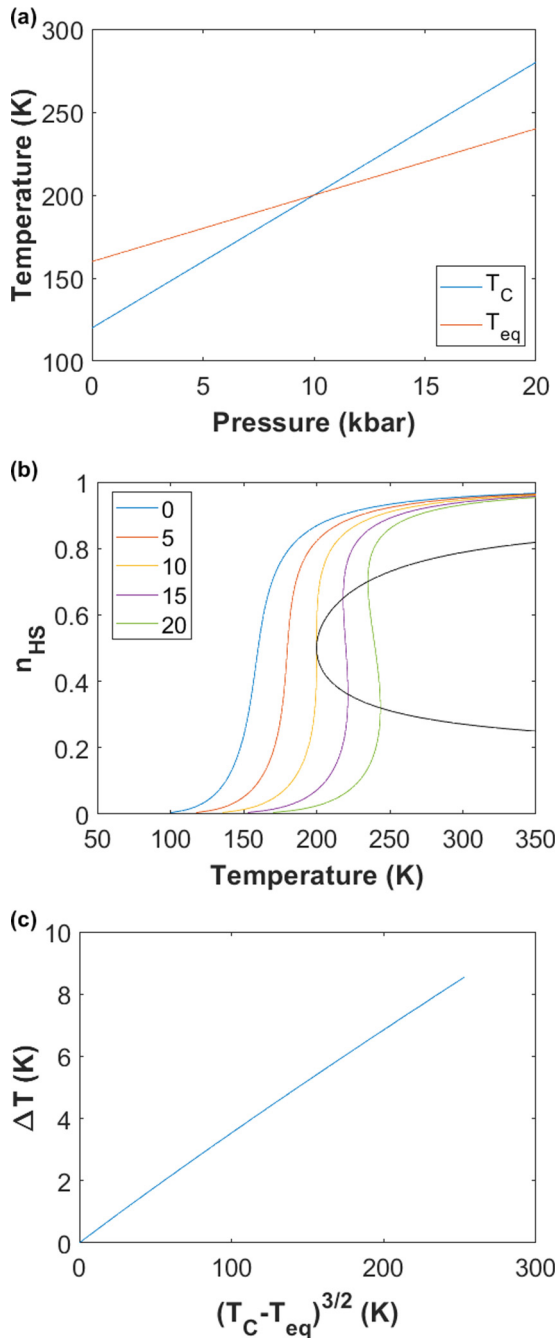
FIG. 3. (a) Phase diagram exhibiting the pressure dependence of the spin transition T_{eq} and the Curie temperature T_C, showing the opposite situation with respect to that of Fig. 2(a). (b) Thermal dependence of the HS fraction under pressure showing a transformation from a gradual to first-order spin transition as the pressure increases. The black curve is the spinodal curve, which delimits the bistable region. (c) The superlinear behavior of the thermal hysteresis width as a function of $(T_C - T_{eq})^{3/2}$ obtained for the curves of (a). The parameter values are $\sqrt{g} = 150$, $\Delta_0 = 400.1$ K, $J_0 = 120$ K, $\alpha = 20.0$ K/kbar, and $\gamma = 8$ K/kbar.

triazole [57,80] and the cooperative Prussian blue analog [58]. It is important to mention that, in the general case, this happens due to further inner degrees of freedom of the molecules (in addition to the volume change), related to the cooperative rotation of the ligands which can cause a structural phase transition, which then leads to different space groups in LS and HS states [82–86].

3. Case $\alpha < \gamma \ln g$

The second interesting case deals with the situation where the intersection between $T_{eq}(P)$ and $T_C(P)$ takes place for negative pressure values. This is possible when the Curie temperature at zero pressure, T_C^0, is greater than T_{eq}^0 and in addition their slopes are in such a way that $\frac{\partial T_{eq}(P)}{\partial P} < \frac{\partial T_C(P)}{\partial P}$. Thus the two lines $T_{eq}(P)$ and $T_C(P)$ move away from each other as the pressure increases, a situation that the reader can easily check. It is then expected that the corresponding thermal dependence of the HS fraction under pressure will show a monotonous increase of the thermal hysteresis width.

B. Case of gradual spin transition at zero pressure: $\delta = 0$ and $T_{eq}^0 > T_C^0$

Here, we study the case of the evolution of the HS fraction of a spin-crossover system, exhibiting a gradual transition at zero applied pressure. For that, the first condition satisfies the relation $T_{eq}^0 > T_C^0$. According to the slopes $\frac{\alpha}{k_B \ln g}$ and γ, the effect of pressure may lead to the emergence of a first-order transition or to maintain the gradual character of the spin transition. Two cases are examined below.

1. Case $\alpha < \gamma \ln g$

In the case where the following condition, $\frac{\partial T_{eq}(P)}{\partial P} < \frac{\partial T_C(P)}{\partial P}$, is realized, one gets the phase diagram of Fig. 3(a), displaying the pressure dependence of $T_{eq}(P)$ and $T_C(P)$ of the current situation. Figure 3(a) already implies the existence of two regions corresponding to (i) $T_{eq}(P) > T_C(P)$, in which the HS fraction exhibits a gradual spin transition (a simple Boltzmann population between two degenerate states), and a second region (ii) for which $T_{eq}(P) < T_C(P)$, where a first-order phase spin transition takes place. According to this statement, there exists a critical pressure $P_C = \frac{k_B(T_{eq}^0 - T_C^0)}{(\gamma - \frac{\alpha}{\ln g})}$ beyond which the thermal hysteresis emerges due to pressure effects. The corresponding thermal dependence of the HS fraction is presented in Fig. 3(b), confirming the above predictions of the phase diagram of Fig. 3(a). Indeed, a gradual spin transition is obtained for $P = 0$ and for all curves below the critical pressure, $P_C \sim 10$ kbar, beyond which first-order spin transition with hysteresis take place. Figure 3(c) summarizes the dependence of the thermal hysteresis width ΔT as a function of the difference $[T_C(P) - T_{eq}(P)]$, confirming the universal law obtained in Fig. 2(c).

2. Case $\alpha > \gamma \ln g$

Finally, for the case $\alpha > \gamma \ln g$, we expect a phase diagram $T-P$ in which the curves of $T_{eq}(P)$ and $T_C(P)$ move away from each other, leading to stabilize the gradual character of the spin transition under pressure.

C. Case $\delta \neq 0$: Pressure-induced reentrant phase transition

Some experimental examples in the literature [62,63,81] have shown that the thermal hysteresis of SCO systems under pressure may show nonmonotonous behavior. For example, by increasing the applied pressure, the thermal hysteresis width first decreases and increases again after some threshold pressure value. This behavior is attributed to the existence of an additional pressure-induced structural phase transition in the SCO material, triggered beyond some threshold pressure value, which leads to significantly changing the material properties. We have seen in Eq. (23) that the simultaneous change under pressure of the elastic constant and the connectivity of the lattice may induce a nonlinear dependence of the Curie temperature with pressure. When $\delta < 0$, this insures that the Curie temperature will go through a maximum for the pressure value $P_C = \frac{2\gamma}{|\delta|}$. On the other hand, since the transition temperature $T_{eq}(P)$ will not be affected by any nonlinear term, we still use $T_{eq}(P) = T_{eq}^0 + \frac{\alpha}{\ln g} P$, where k_B is put equal to 1.

One of the requirements for obtaining the pursued phenomenon is to fulfill two conditions: (i) T_{eq} $(P = 0) > T_C (P = 0)$, ensuring that at zero applied pressure the system shows a gradual spin transition and (ii) a second constraint between the maximum of the Curie temperature and the spin transition temperature $T_C(P^*) > T_{eq}(P^*)$ at the pressure $P^* = \frac{\gamma}{|\delta|}$, also depicted in the phase diagram of Fig. 4(a). The two previous conditions, realized for $T_{eq}^0 > T_C^0$ and $\frac{\gamma}{|\delta|}(\frac{\alpha}{\ln g} + \frac{\gamma}{2}) > (T_{eq}^0 - T_C^0)$, are fulfilled in Fig. 4(a), which was obtained for the parameter values $\sqrt{g} = 150$, $\Delta_0 = 250.5$ K, $J_0 = 23.9$ K, $\alpha = 33.4$ K/kbar, $\gamma = 35.8$ K/kbar, and $\delta = -2.78$ K/kbar^2. There, the first-order spin transition is confined in the region $P^- < P < P^+$, where P^- and P^+ [whose expressions are given in Eq. (A1) of the Appendix] are the solutions of the equation $T_C (P) = T_{eq} (P)$. For $P > P^+$, the gradual spin transition is recovered, leading to reentrant behavior, depicted in Fig. 4(b), in which we also plotted the spinodal curve, representing the trajectories of the upper and lower transition temperatures of the thermal hysteresis, which now shows a closed loop. It is worth noticing that reversing the sign of δ in Eq. (23) would result in the transformation under pressure of a first-order transition to a gradual transition and then to a first-order transition again, which means that the first-order transition will vanish and reappear again for higher pressures. According to the slope of the spin transition temperature $T_{eq} (P)$ with pressure, we could obtain several other situations. Figure 4(c) summarizes the pressure dependence of the upper and lower transition temperatures of the thermal hysteresis, confirming the gradual character of the transition for $P < 2.5$ kbar, which turns to first order in the applied interval $2.5 < P < 17$ kbar before coming back to its initial gradual character for $P > 17$ kbar.

It is worth noticing that reversing the sign of δ in Eq. (23) and choosing the adequate γ value, so as to fulfill the conditions $T_{eq} (P = 0) < T_C (P = 0)$ and $T_C(P^*) > T_{eq}(P^*)$, where $T_C(P^*)$ is the minimum of $T_C (P)$, would result in a reentrant phase transition as depicted in Figs. 5(a) and 5(b). In these conditions, we have the relations $T_{eq}^0 < T_C^0$ and $\frac{\gamma}{|\delta|}(\frac{\alpha}{\ln g} + \frac{\gamma}{2}) < (T_{eq}^0 - T_C^0)$, and increasing the applied pressure transforms
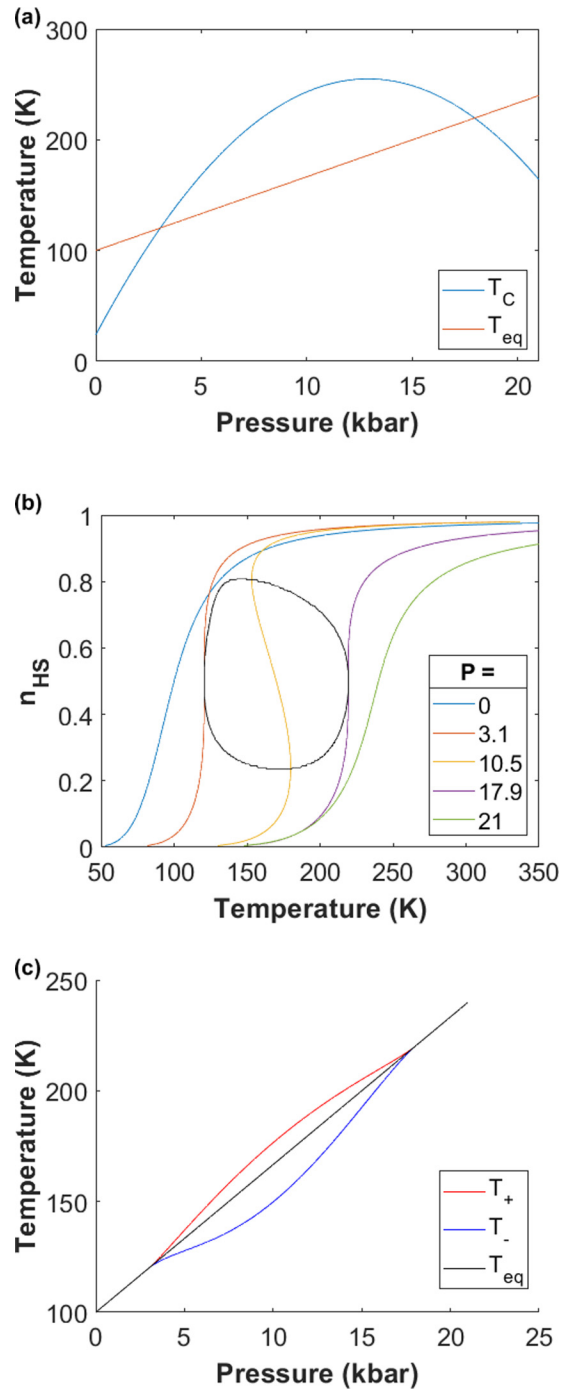

FIG. 4. (a) Pressure dependence of the spin transition temperature T_{eq} and the Curie temperature T_C, showing the existence of three regions: $T_{eq} > T_C$, $T_{eq} < T_C$, and $T_{eq} > T_C$, due to the nonmonotonous character of the Curie temperature with pressure. (b) Associated thermal dependence of the HS fraction for several applied pressure values, going from 0 to 20 kbar, exhibiting a reentrant behavior from gradual to first-order and then to gradual spin transition as P increases. (c) Associated pressure dependence of the spin transition temperature (black curve) and upper (in red) and lower (in blue) switching temperatures of the thermal hysteresis, helping to visualize the observed reentrant phase transition. Parameter values used are $\sqrt{g} = 150$, $\Delta_0 = 250.5$ K, $J_0 = 23.9$ K, $\alpha = 33.4$ K/kbar, $\gamma = 35.8$ K/kbar, and $\delta = -2.78$ K/kbar^2.
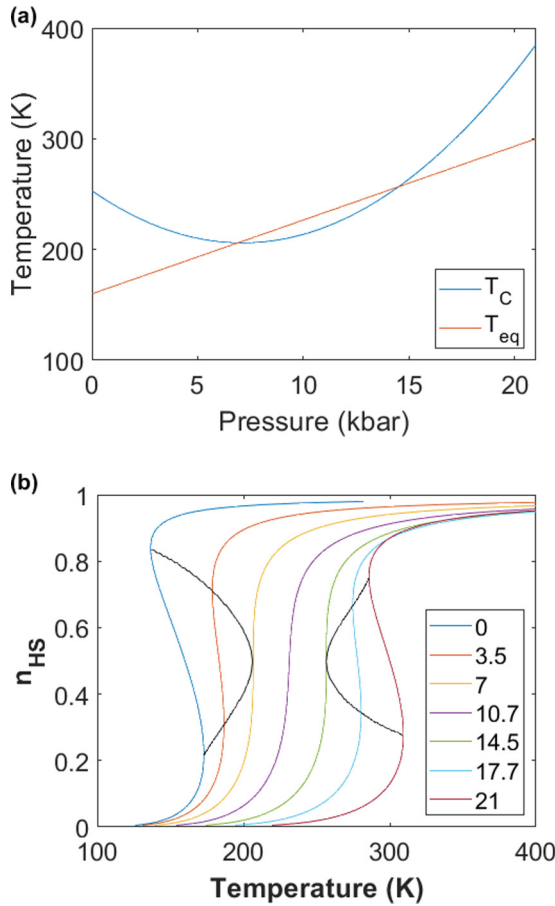
FIG. 5. (a) Pressure dependence of the spin transition temperature T_{eq} and the Curie temperature T_C, showing the existence of three regions: $T_{eq} < T_C$, $T_{eq} > T_C$, and $T_{eq} < T_C$, due to the nonmonotonous pressure dependence of the Curie temperature with pressure. (b) Associated thermal dependence of the HS fraction for several applied pressure values, going from 0 to 21 kbar, exhibiting a reentrant behavior from first-order to gradual and then to first-order spin transition as P increases. The black curves denote the spinodal lines. Parameter values used are $g = 150$, $\Delta_0 = 400.8$ K, $J_0 = 253$ K, $\alpha = 33.4$ K/kbar, $\gamma = -13.2$ K/kbar, and $\delta = 1.857$ K/kbar^2.

the first-order transition to a gradual spin transition, while the first-order transition reappears again for higher pressures. The critical pressures at which the first-order transition vanishes first and reappears again are easily calculated by solving the equation $T_C(P) = T_{eq}(P)$, which leads to $T_C^0 + \gamma P - \frac{|\delta|}{2}P^2 = T_{eq}^0 + \frac{\alpha}{\ln g}P$. The latter has two solutions, P^+ and P^-, whose expressions are given in Eq. (A2) of the Appendix.

IV. CONCLUSION

In summary, in this work, based on the Ising-like description of the SCO phenomenon, we have carried out a general study of the thermal properties of spin-crossover systems under pressure. First, we have derived the well-known phenomenological Ising-like Hamiltonian model from an elastic description of the spin transition lattice taking into account the volume change at the transition. By assuming

a uniform lattice spacing, we can map the elastic model into an Ising-like Hamiltonian with long-range interactions. We have also included the effect of pressure in the elastic model and demonstrated that the latter renormalizes linearly the ligand-field energy and nonlinearly the interactions inside the lattice. We have then investigated several possible effects of pressure on the thermal behavior of the HS fraction. We found that a rich variety of thermal behaviors under pressure can be obtained. According to the initial values of the spin transition temperature T_{eq}^0 and the Curie temperature T_C^0 and their pressure dependences, we developed a general analytical treatment which allows us to predict the thermal behavior of the HS fraction under pressure. Among the obtained results, we quote (i) the simple vanishing of the thermal hysteresis under pressure, (ii) the nonmonotonous increase of the thermal hysteresis under pressure, and (iii) the pressure-induced reentrant-phase transitions originating from the pressure dependence of the interaction parameter, in good agreement with the available data of the literature. Furthermore, the analytical method developed for the prediction of the various pressure influences on the thermal hysteresis, based on the comparison between $T_C(P)$ and $T_{eq}(P)$, is exact, and hence could be easily applied to the resolution of the present model by Monte Carlo simulations, whose preliminary results confirm the present mean-field findings. These results will be published in a separate work with a general resolution of the elastic model under pressure.

APPENDIX

The expressions of the threshold pressures P^+ and P^- delimiting the bistable region (thermal hysteresis area) are

$$P^{\pm} = \frac{(\alpha - \gamma \ln g) \mp \sqrt{(\alpha - \gamma \ln g)^2 + 2|\delta|(T_C^0 - T_{eq}^0)}}{|\delta|}. \tag{A1}$$

The general expressions of the spinodal curves depicted in Figs. 1(a), 2(b), 3(b), 4(b), and 5(b), plotted in the plane $T - m$, are given by

$$k_B T = \frac{-J + 2\gamma\left(\frac{Jm-\Delta}{2m\gamma-\alpha}\right)}{\gamma \frac{\ln\left[\frac{1}{g}\left(\frac{1+m}{1-m}\right)\right]}{2m\gamma-\alpha} + \frac{1}{(m^2-1)}1}. \tag{A2}$$

Using the expressions of T_C^0 and T_{eq}^0, α, γ, δ, Eq. (A2) transforms to

$$k_B T = \frac{\alpha T_C^0}{\gamma \ln\left[\frac{1}{g}\left(\frac{1+m}{1-m}\right)\right] + \frac{(2m\gamma-\alpha)}{(m^2-1)} + T_{eq}^0 \ln(g)}. \tag{A3}$$

[1] E. Coronado, Nat. Rev. Mater. **5**, 87 (2019).

[2] *Spin Crossover in Transition Metal Compounds I*, edited by P. Gütlich and H. A. Goodwin, Topics in Current Chemistry Vol. 233 (Springer, Berlin, 2004).

[3] P. Gütlich, A. Hauser, and H. Spiering, Angew. Chem., Int. Ed. Engl. **33**, 2024 (1994).

[4] C. P. Köhler, R. Jakobi, E. Meissner, L. Wiehl, H. Spiering, and P. Gütlich, J. Phys. Chem. Solids, **51**, 239 (1990).

[5] E. König, in *Complex Chemistry*, Structure and Bonding Vol. 76 (Springer, Berlin, 1991).

[6] S.-I. Ohkoshi, K. Imoto, Y. Tsunobuchi, S. Takano, and H. Tokoro, Nat. Chem. **3**, 564 (2011).

[7] T. D. Oke, F. Hontinfinde, and K. Boukheddaden, Eur. Phys. J. B **86**, 271 (2013).

[8] T. D. Oke, F. Hontinfinde, and K. Boukheddaden, Appl. Phys. A **120**, 309 (2015).

[9] E. König, Struct. Bonding (Berlin, Ger.) **76**, 51 (1991).

[10] A. Hauser, J. Jeftić, H. Romstedt, R. Hinek, and H. Spiering, Coord. Chem. Rev. **190**, 471 (1999).

[11] T. Kambara, J. Phys. Soc. Jpn. **49**, 1806 (1980).

[12] N. Sasaki, J. Chem. Phys. **74**, 3472 (1981).

[13] S. W. Biernacki and B. Clerjaud, Phys. Rev. B **72**, 024406 (2005).

[14] G. D'Avino, A. Painelli, and K. Boukheddaden, Phys. Rev. B **84**, 104119 (2011).

[15] M. Castro, O. Roubeau, L. Piñeiro-López, J. A. Real, and J. A. Rodríguez-Velamazán, J. Phys. Chem. C **119**, 17334 (2015).

[16] Y. De Gaetano, E. Jeanneau, A. Y. Verat, L. Rechignat, A. Bousseksou, and G. S. Matouzenko, Eur. J. Inorg. Chem. **2013**, 1015 (2013).

[17] S. Pillet, J. Hubsch, and C. Lecomte, Eur. Phys. J. B **38**, 541 (2004).

[18] S. Gawali-Salunke, F. Varret, I. Maurin, C. Enachescu, M. Malarova, K. Boukheddaden, E. Codjovi, H. Tokoro, S. Ohkoshi, and K. Hashimoto, J. Phys. Chem. B **109**, 8251 (2005).

[19] V. Mishra, R. Mukherjee, J. Linares, C. Balde, C. Desplanches, J. F. Letard, E. Collet, L. Toupet, M. Castro, and F. Varret, Inorg. Chem. **47**, 7577 (2008).

[20] F. Varret, C. Chong, A. Goujon, and K. Boukheddaden, J. Phys.: Conf. Ser. **148**, 012036 (2009).

[21] A. Goujvon, F. Varret, K. Boukheddaden, C. Chong, J. Jeftić, Y. Garcia, A. D. Naik, J. C. Ameline, and E. Collet, Inorg. Chim. Acta **361**, 4055 (2008).

[22] C. Chong, H. Mishra, K. Boukheddaden, S. Denise, G. Bouchez, E. Collet, J.-C. Ameline, A. D. Naik, Y. Garcia, and F. Varret, J. Phys. Chem. B **114**, 1975 (2010).

[23] A. Slimani, F. Varret, K. Boukheddaden, C. Chong, H. Mishra, J. Haasnoot, and S. Pillet, Phys. Rev. B **84**, 094442 (2011).

[24] F. Varret, A. Slimani, K. Boukheddaden, C. Chong, H. Mishra, E. Collet, J. Haasnoot, and S. Pillet, New J. Chem. **35**, 2333 (2011).

[25] C. Chong, A. Slimani, F. Varret, K. Boukheddaden, E. Collet, J. C. Ameline, R. Bronisz, and A. Hauser, Chem. Phys. Lett. **504**, 29 (2011).

[26] Y. Garcia, F. Robert, A. D. Naik, G. Zhou, B. Tinant, K. Robeyns, S. Michotte, and L. Piraux, J. Am. Chem. Soc. **133**, 15850 (2011).

[27] B. Benaicha, K. Van Do, A. Yangui, N. Pittala, A. Lusson, M. Sy, G. Bouchez, H. Fourati, C. J. Gómez-García, S. Triki, and K. Boukheddaden, Chem. Sci. **10**, 6791 (2019).

[28] C. Lochenie, K. Schötz, F. Panzer, H. Kurz, B. Maier, F. Puchtler, S. Agarwal, A. Köhler, and B. Weber, J. Am. Chem. Soc. **140**, 700 (2018).

[29] J. Yuan, S.-Q. Wu, M.-J. Liu, O. Sato, and H.-Z. Kou, J. Am. Chem. Soc. **140**, 9426 (2018).

[30] K. Boukheddaden, M. H. Ritti, G. Bouchez, M. Sy, M. M. Dîrtu, M. Parlier, J. Linares, and Y. Garcia, J. Phys. Chem. C **122**, 7597 (2018).

[31] J. Linares, E. Codjovi, and Y. Garcia, Sensors **12**, 4479 (2012).

[32] V. Ksenofontov, G. Levchenko, H. Spiering, P. Gütlich, J. F. Létard, Y. Bouhedja, and O. Kahn, Chem. Phys. Lett. **294**, 545 (1998).

[33] C.-M. Jureschi, I. Rusu, E. Codjovi, J. Linares, Y. Garcia, and A. Rotaru, Phys. B (Amsterdam, Neth.) **449**, 47 (2014).

[34] C.-M. Jureschi, J. Linares, A. Boulmaali, P. R. Dahoo, A. Rotaru, and Y. Garcia, Sensors **16**, 187 (2016).

[35] P. S. Vallone, A. N. Tantillo, A. M. dos Santos, J. J. Molaison, R. Kulmaczewski, A. Chapoy, P. Ahmadi, M. A. Halcrow, and K. G. Sandeman, Adv. Mater. **31**, 1807334 (2019).

[36] P. Lloveras, E. Stern-Taulats, M. Barrio, J. L. Tamarit, S. Crossley, W. Li, V. Pomjakushin, A. Planes, L. Manosa, N. D. Mathur, and X. Moya, Nat. Commun. **6**, 8801 (2015).

[37] P. J. von Ranke, Appl. Phys. Lett. **110**, 181909 (2017).

[38] K. G. Sanderman, APL Mater. **4**, 111102 (2016).

[39] H. J. Shepherd, P. Rosa, L. Vendier, N. Casati, J. F. Létard, A. Bousseksou, P. Guionneau, and G. Molnar, Phys. Chem. Chem. Phys. **14**, 5265 (2012).

[40] H. G. Drickamer, C. W. Frank, and C. P. Slichter, Proc. Natl. Acad. Sci. USA **69**, 933 (1972).

[41] D. M. Adams, G. J. Long, and A. D. Williams, Inorg. Chem. **21**, 1049 (1982).

[42] H. J. Shepherd, C. Bartual-Murgui, G. Molnár, J. A. Real, M. C. Munõz, L. Salmon, and A. Bousseksou, New J. Chem. **35**, 1205 (2011).

[43] G. Molnár, T. Kitazawa, L. Dubrovinsky, J. J. McGarvey, and A. Bousseksou, J. Phys.: Condens. Matter **16**, S1129 (2004).

[44] G. Molnár, V. Niel, J. A. Real, L. Dubrovinsky, A. Bousseksou, and J. J. McGarvey, J. Phys. Chem. B **107**, 3149 (2003).

[45] E. D. Loutete-Dangui, F. Varret, E. Codjovi, P. R. Dahoo, H. Tokoro, S. Ohkoshi, C. Eypert, J.-F. Létard, J. M. Coanga, and K. Boukheddaden, Phys. Rev. B **75**, 184425 (2007).

[46] G. G. Levchenko, G. V. Bukin, A. B. Gaspar, and J. A. Real, Russ. J. Phys. Chem. A **83**, 951 (2009).

[47] M.-L. Boillot, J. Zarembowitch, J.-P. Itié, A. Polian, E. Bourdet, and J. G. Haasnoot, New J. Chem. **26**, 313 (2002).

[48] E. Codjovi, N. Menéndez, J. Jeftic, and F. Varret, C. R. Acad. Sci., Ser. IIc: Chim. **4**, 181 (2001).

[49] A. Rotaru, F. Varret, E. Codjovi, K. Boukheddaden, J. Linares, A. Stancu, P. Guionneau, and J.-F. Létard, J. Appl. Phys. **106**, 053515 (2009).

[50] A. Rotaru, J. Linares, F. Varret, E. Codjovi, A. Slimani, R. Tanasa, C. Enachescu, A. Stancu, and J. Haasnoot, Phys. Rev. B **83**, 224107 (2011).

[51] S. Usha, R. Srinivasan, and C. N. R. Rao, Chem. Phys. **100**, 447 (1985).

[52] J. Jeftic, R. Hinek, S. C. Capelli, and A. Hauser, Inorg. Chem. **36**, 3080 (1997).

[53] V. Ksenofontov, H. Spiering, A. Schreiner, G. Levchenko, H. A. Goodwin, and P. Gütlich, J. Phys. Chem. Solids **60**, 393 (1999).

[54] V. Niel, M. C. Muõz, A. B. Gaspar, A. Galet, G. Levchenko, and J. A. Real, Chem. - Eur. J. **8**, 2446 (2002).

[55] T. Granier, B. Gallois, J. Gaultier, J. A. Real, and J. Zarembowitch, Inorg. Chem. **32**, 5305 (1993).

[56] P. Guionneau, C. Brigouleix, Y. Barrans, A. E. Goeta, J.-F. Létard, J. A. K. Howard, J. Gaultier, and D. Chasseau, C. R. Acad. Sci., Ser. IIc: Chim. **4**, 161 (2001).

[57] P. Guionneau, M. Marchivie, Y. Garcia, J. A. K. Howard, and D. Chasseau, Phys. Rev. B **72**, 214408 (2005).

[58] H. J. Shepherd, S. Bonnet, P. Guionneau, S. Bedoui, G. Garbarino, W. Nicolazzi, A. Bousseksou, and G. Molnár, Phys. Rev. B **84**, 144107 (2011).

[59] A. Sava, C. Enachescu, A. Stancu, K. Boukheddaden, E. Codjovi, I. Maurin, and F. Varret, J. Optoelectron. Adv. Mater. **5**, 977 (2003).

[60] D. Pinkowicz, M. Rams, M. Misek, K. V. Kamenev, H. Tomkowiak, A. Katrusiak, and B. Sieklucka, J. Am. Chem. Soc. **137**, 8795 (2016).

[61] H. Spiering, K. Boukheddaden, J. Linarès, and F. Varret, Total free energy of a spin crossover molecular system, Phys. Rev. B **70**, 184106 (2004).

[62] R. Lesquezec (private communication, unpublished).

[63] S. Triki (private communication, unpublished).

[64] S. Wang, S. Hirai, M. C. Shapiro, S. C. Riggs, T. H. Geballe, W. L. Mao, and I. R. Fisher, Phys. Rev. B **87**, 054104 (2013).

[65] E. Tailleur, M. Marchivie, J.-P. Itié, P. Rosa, N. Daro, and P. Guionneau, Chem. Eur. J. **24**, 14495 (2018).

[66] P. Guionneau and E. Collet, Piezo- and photo-crystallography applied to spin-crossover materials, in *Spin-Crossover Materials: Properties and Applications*, edited by M. A. Halcrow (John Wiley & Sons Ltd, Oxford, UK, 2013), Chap. 20, p. 507.

[67] Y. Wang, Z. Zhou, T. Wen, Y. Zhou, N. Li, F. Han, Y. Xiao, P. Chow, J. Sun, M. Pravica, A. L. Cornelius, W. Yang, and Y. Zhao, J. Am. Chem. Soc. **138**, 15751 (2016).

[68] K. Boukheddaden, Phys. Rev. B **88**, 134105 (2013).

[69] M. Nishino, K. Boukheddaden, and S. Miyashita, Phys. Rev. B **79**, 012409 (2009).

[70] S. Bonhommeau, G. Molnar, M. Goiran, K. Boukheddaden, and A. Bousseksou, Phys. Rev. B **74**, 064424 (2006).

[71] C. P. Slichter and H. G. Drickamer, J. Chem. Phys. **56**, 2142 (1972).

[72] E. Meissner, H. Köppen, H. Spiering, and P. Gütlich, Chem. Phys. Lett. **95**, 163 (1983).

[73] H. Spiering, E. Meissner, H. Köppen, E. W. Müller, and P. Gütlich, Chem. Phys. **68**, 65 (1982).

[74] P. Adler, L. Wiehl, E. Meissner, C. P. Köhler, H. Spiering, and P. Gütlich, J. Phys. Chem. Solids **48**, 517 (1987).

[75] H. Köppen, E. Meissner, L. Wiehl, H. Spiering, and P. Gütlich, Hyperfine Interact. **52**, 29 (1989).

[76] S. Klokishner, J. Linares, and F. Varret, Chem. Phys. **255**, 317 (2000).

[77] Y. Konishi, H. Tokoro, M. Nishino, and S. Miyashita, Phys. Rev. Lett. **100**, 067206 (2008).

[78] L. Stoleriu, C. Enachescu, A. Stancu, and A. Hauser, IEEE Trans. Magn. **44**, 3052 (2008).

[79] A. Rotaru, J. Linares, E. Codjovi, J. Nasser, and A. Stancu, J. Appl. Phys. **103**, 07B908 (2008).

[80] D. Taniguchi, J. Okabayashi, and C. Hotta, Phys. Rev. B **96**, 174104 (2017).

[81] K. Boukheddaden, J. Linares, H. Spiering, and F. Varret, Eur. Phys. J. B **15**, 317 (2000).

[82] Y. Garcia, V. Ksenofontov, G. Levchenko, G. Schmitt, and P. Gütlich, J. Phys. Chem. B **104**, 5045 (2000).

[83] E. König, G. Ritter, J. Waigel, and H. A. Goodwin, J. Chem. Phys. **83**, 3055 (1985).

[84] Y. Garcia, P. van Koningsbruggen, R. Lapuyade, L. Fournès, L. Rabardel, O. Kahn, V. Ksenofontov, G. Levchenko, and P. Gütlich, Chem. Mater. **10**, 2426 (1998).

[85] Y. Garcia, V. Ksenofontov, and P. Gütlich, Hyperfine Interact. **139**, 543 (2002).

[86] P. Guionneau, J. F. Létard, D. S. Yufit, D. Chasseau, G. Bravic, A. E. Goeta, J. A. K. Howard, and O. Kahn, J. Mater. Chem. **9**, 985 (1999).